European Journal of Medicinal Chemistry 78 (2014) 455–467

Contents lists available at ScienceDirect

European Journal of Medicinal Chemistry

journal homepage: http://www.elsevier.com/locate/ejmech

Original article

Design, synthesis and biological evaluation of novel tetrahydroacridine pyridine- aldoxime and -amidoxime hybrids as efficient uncharged reactivators of nerve agent-inhibited human acetylcholinesterase

Maria Kliachyna [a], Gianluca Santoni [b], Valentin Nussbaum [a], Julien Renou [c], Benoit Sanson [b], Jacques-Philippe Colletier [b], Mélanie Arboléas [d], Mélanie Loiodice [d], Martin Weik [b,*], Ludovic Jean [c], Pierre-Yves Renard [c,*], Florian Nachon [b,d,*], Rachid Baati [a,*]

[a] Université de Strasbourg, Faculté de Pharmacie, CNRS/ UMR 7199 BP 24, 74 route du rhin 67401 Illkirch, France
[b] Commissariat à l'Energie Atomique, Institut de Biologie Structurale, F-38054 Grenoble; CNRS, UMR5075, F-38027 Grenoble; Université Joseph Fourier, F-38000, Grenoble, France
[c] Normandie University, COBRA, UMR 6014 and FR 3038; University of Rouen; INSA of Rouen; CNRS, 1 rue Tesniere 76821 Mont-Saint-Aignan, Cedex, France
[d] Département de Toxicologie, Institut de Recherche Biomédicale des Armées BP7391993 Brétigny/s/Orge, France

ARTICLE INFO

Article history:
Received 27 November 2013
Received in revised form
3 March 2014
Accepted 14 March 2014
Available online 15 March 2014

Keywords:
Organophosphorus nerve agents
Reactivation of acetylcholinesterase
Pyridinaldoximes
Oximes
Hybrids
Tacrine

ABSTRACT

A series of new uncharged functional acetylcholinesterase (AChE) reactivators including heterodimers of tetrahydroacridine with 3-hydroxy-2-pyridine aldoximes and amidoximes has been synthesized. These novel molecules display *in vitro* reactivation potencies towards VX-, tabun- and paraoxon-inhibited human AChE that are superior to those of the mono- and bis-pyridinium aldoximes currently used against nerve agent and pesticide poisoning. Furthermore, these uncharged compounds exhibit a broader reactivity spectrum compared to currently approved remediation drugs.

1. Introduction

Organophosphorus compounds (OP) include the extremely toxic chemical warfare agents (CWA) (sarin, soman, cyclosarin, tabun, methylphosphonothioate VX) and pesticides (paraoxon, parathion, tetraethyl pyrophosphate (TEPP)) (Fig. 1). Their acute toxicity results from the irreversible inhibition of acetylcholinesterase (AChE) through phosphylation of its catalytic serine [1]. Accumulation of neurotransmitter acetylcholine (ACh) at cholinergic synapses ensues, leading to nervous and respiratory failures. Depending on the class of OP and on the administrated dose, death can occur within minutes [2].

Due to the similarity between the chemical precursors of CWA and pesticides, and to the relatively simple chemistry involved in their synthesis, efforts to control the proliferation of these agents have proved of limited success [3]. Illustrative examples include the terrorist attack in the Tokyo subway in 1995, the bombing of Kurd civilians during the Iraq–Iran war in 1988, and that of civilians in Syria, as reported in August 2013. Additionally, despite the international efforts aimed at regulating and lessening the use of these environmentally toxic compounds, ca. 100 different OP are still used intensively as pest control agents, with only anecdotal monitoring. This results in about 3,000,000 acute intoxications per year, 200,000 of which lead to death [4,5]. Therefore, the development of effective measures to counteract OP poisoning remains a challenging issue to protect and treat both civilian and military populations [6].

* Corresponding authors.
E-mail addresses: martin.weik@ibs.fr (M. Weik), pierre-yves.renard@univ-rouen.fr (P.-Y. Renard), florian@nachon.net (F. Nachon), rachid.baati@unistra.fr (R. Baati).

http://dx.doi.org/10.1016/j.ejmech.2014.03.044
0223-5234/

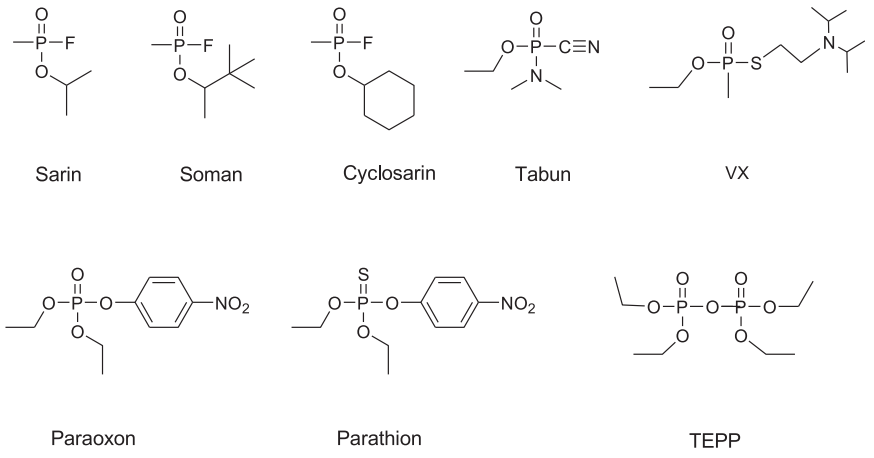

Fig. 1. Structures of organophosphorus CWA and pesticides.

The current treatment against OP poisoning consists in the administration of a combination of atropine (antimuscarinic agent) and diazepam (anticonvulsant drug), to limit convulsions, and of a standard pyridinium oxime (pralidoxime, trimedoxime, HI-6, obidoxime, and HLö-7, Fig. 2) to reactivate AChE. Oximes exert their action on OP-inhibited AChE by attacking the phosphorus atom of the phosphylated serine, yielding to the removal of the phosphonate and recovery of the enzyme's catalytic activity. To this end, pyridinium oximes must display high nucleophilicity, which is generally attained by the formation of an oximate anion at physiological pH. As of today, however, not a single oxime has proven equally effective against all types of OP-inhibited AChE, and most are ineffective for the reactivation of tabun-inhibited hAChE [6].

Another weakness of currently approved pyridinium aldoximes is their difficulty in crossing the blood–brain barrier (BBB) owing to the permanent charge carried by the oximate [7]. For example, it was estimated using *in vivo* rat brain microdialysis coupled with HPLC/UV, that the BBB penetration of the most commonly used oxime, 2-PAM, is only 10% [8]. Therefore, oximes reactivating AChE in the peripheral nervous system are not effective in the brain and, consequently, do not protect against the neurological effects of OP-exposure.

To overcome this obstacle, we recently reported the synthesis of a series of uncharged oxime-based compounds, both able to cross the BBB and to reactivate OP-inhibited AChE in the CNS [6]. Monoisonitrosoacetone (MINA) and diacetylmonooxime (DAM) respectively bearing the α-ketoaldoxime and ketoxime moieties (Fig. 3) were also reported to cross the BBB, yet their *in vitro* reactivation potency towards OP-inhibited AChE was lower than that exhibited by 2-PAM [9]. Connection of an α-ketoaldoxime function to a piperidine-derived peripheral site ligand (PSL) allowed increasing the affinity for AChE, resulting in higher reactivation rates of sarin- and VX- inhibited AChE. Yet, these compounds were still less efficient than currently used pyridinium oximes towards the latter, and totally inefficient towards tabun-inhibited AChE [10]. Hydroxyimino acetamides **1a**–**b** showed *in vitro* reactivation efficacy superior to MINA and DAM, but remained less effective than 2-PAM, except for cyclosarin [11]. Likewise, amidine-oxime reactivators **2a,b** were less potent than 2-PAM in reactivating AChE *in vitro* [12]. Low reactivation potency of these new uncharged reactivators is likely due to their higher pKa, which results in inefficient deprotonation at physiological pH and thus, in a reduced nucleophilicity (for instance, for MINA, pKa = 8.3) [13].

Recently we found that 3-hydroxy-2-pyridine aldoximes **3** and amidoxime **4** (Fig. 4) exhibited high reactivation first order rate constant towards VX-inhibited hAChE ($k_r = 0.5 \pm 0.1$ min^{-1} and 0.08 ± 0.1 min^{-1}, respectively) [14,15], *i.e.* values either similar or one order of magnitude larger than that displayed by 2-PAM ($k_r = 0.06 \pm 0.01$ min^{-1}). Owing to the lower affinity of **3** and **4** for VX-hAChE (second order reactivation rate constants $k_{r2} = k_r/K_D$ are 0.015 and 0.0026 mM^{-1} min^{-1} for **3** and **4**, respectively, to compare to 0.28 mM^{-1} min^{-1} for 2-PAM), much higher concentrations are however required to reach the desirable reactivation of the enzyme.

We have shown that connection of 3-hydroxy-2-pyridinaldoxime reactivators with a PSL ligand, such as phenyltetrahydroisoquinoline (PIQ) [16], results in a dramatically improved affinity for the enzyme and, consequently, in increased

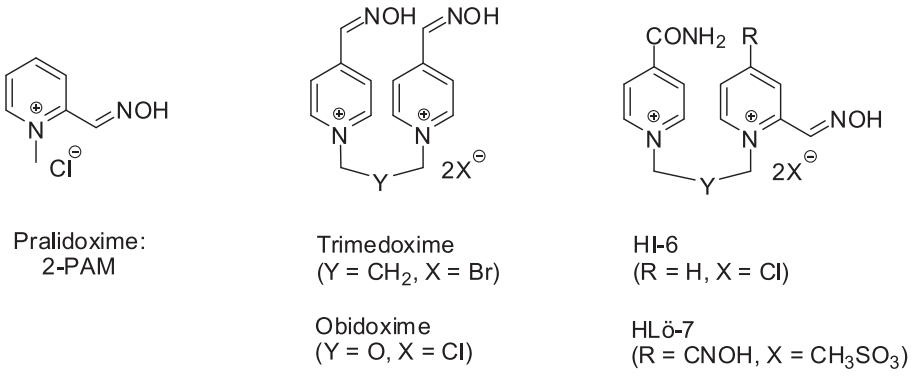

Fig. 2. Structures of developed pyridinium aldoxime reactivators.

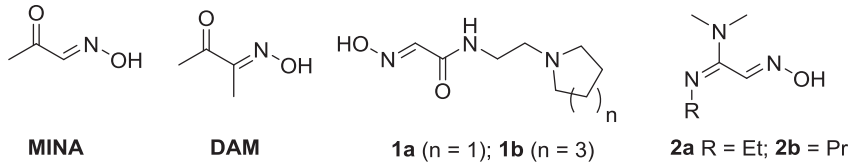

Fig. 3. Neutral reactivators: α-ketoaldoximes, ketoxime, hydroxyimino acetamides, and amidine-oximes.

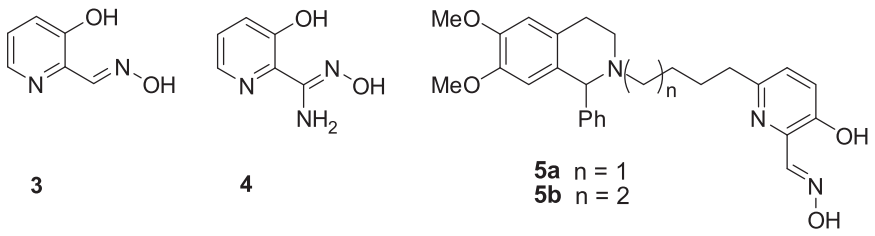

Fig. 4. 3-hydroxy-2-pyridine aldoxime, 3-hydroxy-2-pyridine amidoxime, and phenyl-tetrahydroisoquinoline-3-hydroxy-2-pyridine aldoxime AChE reactivators.

reactivation potency towards OP-inhibited hAChE [17]. Recently, similar beneficial effects have been reported for tryptoline-3-hydroxypyridine-2-aldoxime hybrids for the reactivation of OP-inhibited h-BChE [17c]. PIQ-functionalized 3-hydroxy-2-pyridine aldoximes indeed displayed reactivation potency either equalling or exceeding those of HI-6 and obidoxime. For example, **5a** was 2.3 and 2.8 times more efficient than obidoxime and HI-6, respectively, and 5 times more potent than trimedoxime, the best known reactivator of tabun-inhibited hAChE ($k_{r2} = 3.4$ mM^{-1} min^{-1} for **5a**, as compared to 0.7 mM^{-1} min^{-1} for trimedoxime).

One of the important drawbacks when using pyridinium aldoximes (especially for pyridinium-4-aldoximes) is that the

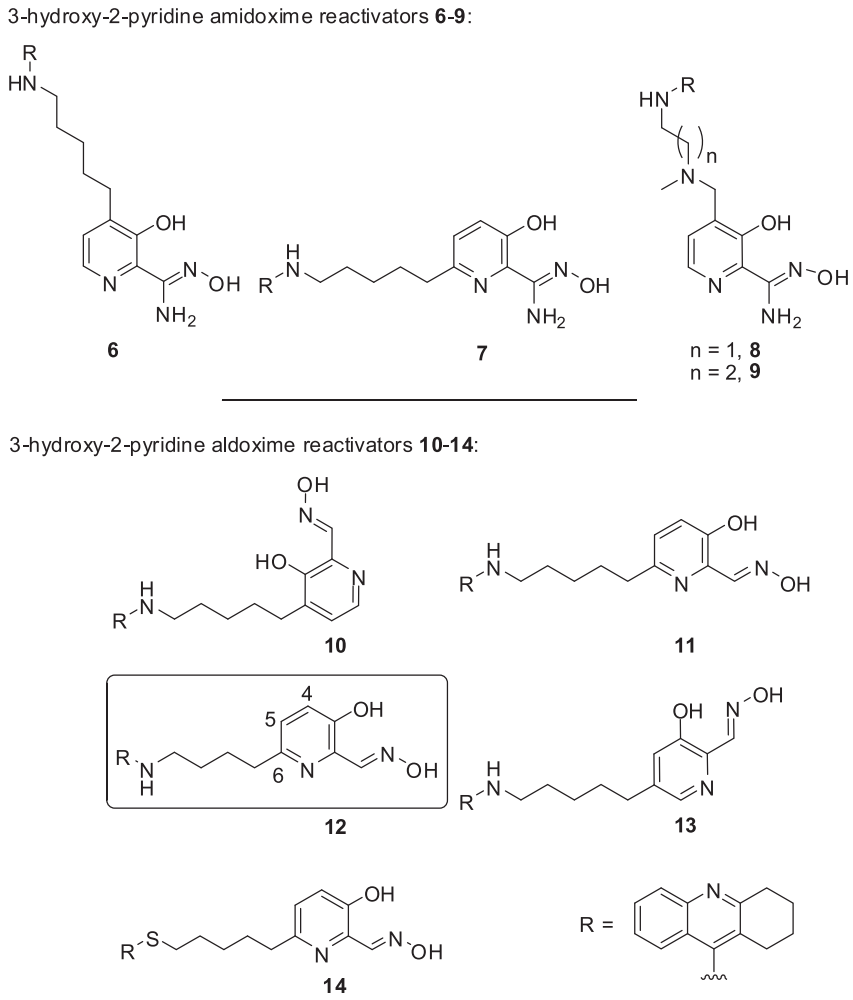

Fig. 5. Structures of novel uncharged AChE hybrid reactivators investigated.

Fig. 6. General structure of targeted hetero-bifunctional reactivators.

reactivation products, phosphyloximes, can themselves display high affinity for the enzyme, and thus prolong AChE inhibition (recapture phenomenon) [18]. In the case of oximes **3**, **5a**, **5b**, as well as in that of amidoxime **4**, the presence of the 3-OH group in α-position of the oxime/amidoxime moiety allows subsequent intramolecular cyclisation, resulting in isoxasole formation and thus in the bypass of this possible complication [14,15].

In the following, we describe the rational design, synthesis and *in vitro* evaluation of a new class of uncharged reactivator molecules. Their design is based on a 1,2,3,4-tetrahydroacridine (tacrine) substructure, able to bind to the peripheral site of AChE [19,20], coupled with various linkers to either 3-hydroxy-2-pyridine aldoxime or 3-hydroxy-2-pyridine amidoxime (Fig. 5).

2. Results and discussion

2.1. Rational design of bifunctional reactivator molecules

Acetylcholinesterase (AChE) features an active site buried at the bottom of a deep and narrow gorge [21]. At the entrance of the latter, a peripheral binding site serves as a transient binding location for substrates and products *en route* to/from the active site [22], but also as an anchor point for ligands [23]. Bifunctional inhibitors have been developed that display higher affinity, and which are based on two moieties binding at either site that are connected by a flexible linker [19,20,24]. By analogy, we designed bifunctional reactivators that comprise a peripheral site ligand (PSL) connected to a reactivator function by a covalent linker (Fig. 6). In addition to increasing the affinity of the reactivator for the enzyme, the use of a PSL further allows preventing unproductive binding to the active site as it was, for example, observed with 2-PAM [25].

In practice, we used as a starting model the X-ray crystal structure of *Torpedo californica* (*Tc*)AChE in complex with a bis-tacrine inhibitor [19], which allowed predicting how the tacrine moiety would bind to the peripheral site. Obviously, the length of the linker had to be optimized so that the oxime moiety could approach the enzyme's phosphylated serine without unbinding from the peripheral site. *In silico* optimization of the linker-length was performed to maximize the reactivation potency of the bifunctional reactivators, and is described in Section 3.

3. Synthesis of the hybrid molecules

3.1. Synthesis of 1,2,3,4-tetrahydro-9-aminoacridine α-hydroxypyridine amidoximes

The 4-substituted α-hydroxypyridine amidoxime **6** was synthesized starting from commercially available 3-hydroxy-2-cyanopyridine **16** (Scheme 1). The introduction of the *ortho*-directing *N*-(diethylamino)carbamate group (both as ortho directing group for the metallation, and as further phenol protecting group) was achieved in standard conditions allowing to obtain compound **17** with a good yield (95%). Subsequent *ortho*-lithiation and substitution with iodine gave the key building block **18**. The Sonogashira coupling with alkyne **19** [26] proceeded cleanly and allowed producing the hybrid compound **20** with 87% yield. Reduction of the alkyne **20** in the presence of Pd/C yielded the corresponding saturated compound **21**. Attempts to selectively deprotect the *N*-(diethylamino)carbamate group of **21** in either acidic or basic conditions proved unsuccessful, due to the competing hydrolysis or degradation of the cyano group. After a set of screening conditions, this critical reaction was successfully achieved upon the treatment of **21** with a large excess (30 equiv.) of hydroxylamine. Under these conditions, the *N*-(diethylamino)carbamate was removed in a *one-pot* process, and the cyano group was concomitantly converted to the desired amidoxime **6**. Thus, the final hybrid molecule **6** was synthesized in a convergent 5-steps protocol with 13% overall yield.

The synthesis of α-hydroxyamidoxime tetrahydroacridine conjugate **7** is shown in Scheme 2. It differs from that of conjugate **6** in that the substitution on the pyridine ring was performed using the optimized modular approach described previously for the Sonogashira coupling of bromopyridine **22** [27] with alkyne **19** (Scheme 2). Indeed, this coupling worked nicely and gave **23** in excellent yield (86%). The *one-pot* alkyne reduction and *O*-debenzylation proceeded cleanly to give nitrile **24**, which was directly reacted

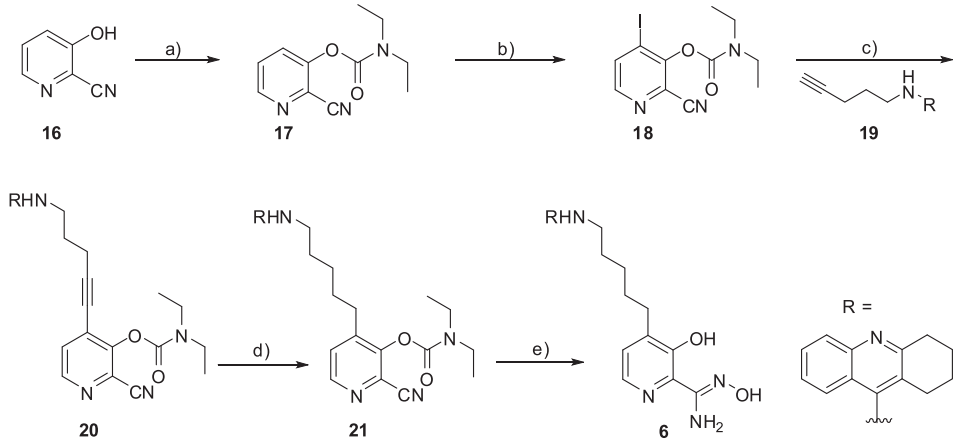

Reagents and conditions: a) *N*-diethylamino carbamate, pyridine, 0°C, **95%**; b) THF, *n*-BuLi, -78°C, then I_2, **48%**; c) **19**, $Pd(PPh_3)_4$, CuI, Et_3N, THF, 20 °C, **87%**; d) H_2, Pd/C, EtOAc, **99%**; e) $NH_2OH.HCl$, pyridine, EtOH reflux, **32 %**

Scheme 1. Synthesis of amidoxime **6**.

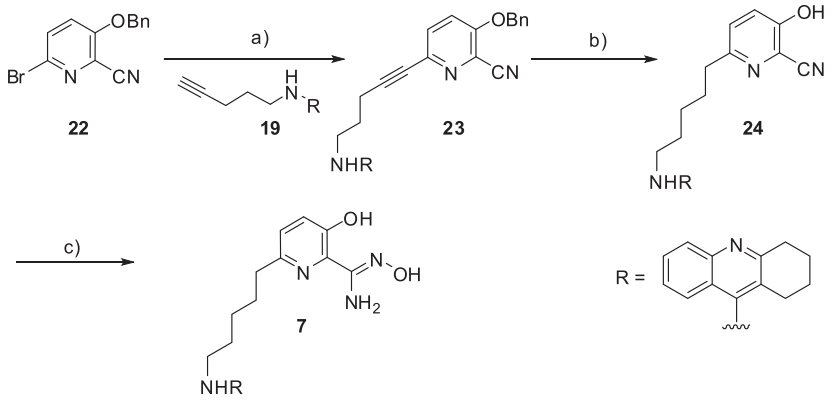

Reagents and conditions: a) **19**, $Pd(PPh_3)_4$, CuI, Et_3N, THF, 20 °C, **86%**; b) H_2, $Pd(OH)_2$/C, MeOH, **80%**; c) $NH_2OH.HCl$, Na_2CO_3, EtOH, H_2O, **65%**.

Scheme 2. Synthesis of amidoxime **7**.

with excess of hydroxylamine hydrochloride to give expected amidoxime **7** with 45% overall yield over the 3 steps.

Docking studies (unpublished results) suggested that the presence of a tertiary amine in the linker could increase the affinity of the molecule for AChE -and thus presumably enhance its reactivation efficacy -owing to the amine protonation at physiological pH that would allow cation-π interaction with the tyrosine residues in AChE gorge [28]. To verify this hypothesis, we therefore prepared hybrids **8** and **9**. The synthesis of these α-hydroxypyridine amidoxime hybrids connected with tetrahydroacridine by *N*–Me linker was based on the reductive amination of aldehyde **25** (obtained by *ortho*-lithiation and subsequent formylation of **17**) with amines **26** and **27** [29] (Scheme 3). The treatment of **28** and **29** with excess hydroxylamine gave α-hydroxypyridine amidoximes **8** and **9** in 13% and 19% overall yields, respectively, over the 3 steps syntheses.

3.2. Synthesis of 1,2,3,4-tetrahydro-9-aminoacridine α-hydroxypyridine aldoximes

For the synthesis of α-hydroxypyridine oxime hybrids, we first started with the synthesis of 3-hydroxypyridine aldoxime with the linker in position 4, using the common intermediate **21**. For these molecules, we privileged the *one-pot* carbamate group removal and methanolysis of cyano- function to give methyl ester **30** with a reasonable yield of 42% (Scheme 4). Next, **30** was converted to **31** *via* a three-step [17] sequence that included: (a) TBDMS protection of phenol function; (b) reduction of methyl ester to aldehyde with DIBAL-H; (c) and subsequent deprotection of the silyl-oxy function using TBAF (33% over three steps). Reaction of the resulting aldehyde **31** with NH_2OH resulted in the formation of the desired pyridinaldoxime **10**, with 7% overall yield.

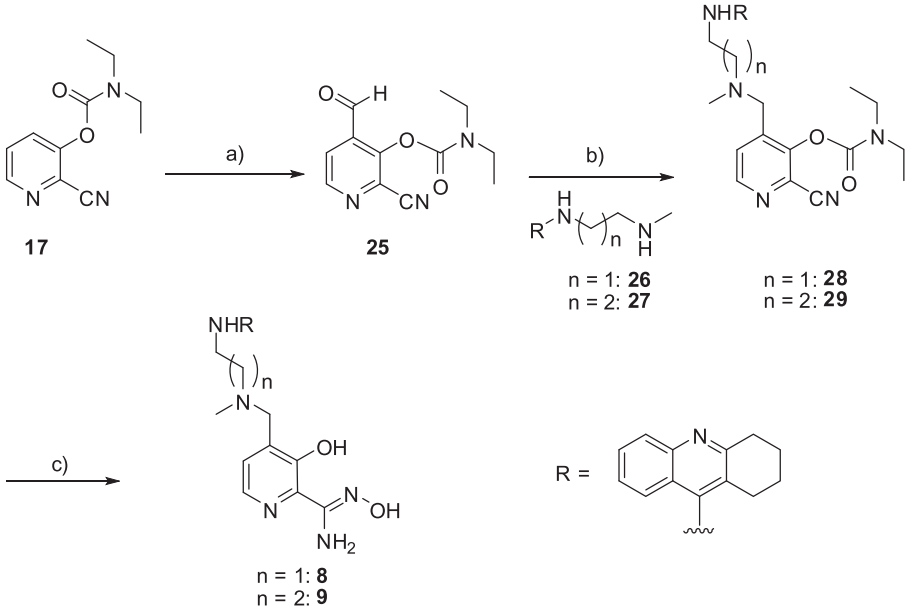

Reagents and conditions: a) *n*-BuLi, THF, -78°C, then DMF, **53%**; b) **26** or **27**, $NaBH(OAc)_3$, THF, 20 °C, **75-99%**; c) $NH_2OH.HCl$, pyridine, EtOH, reflux, **32-37%**.

Scheme 3. Synthesis of amidoximes **8** and **9**.

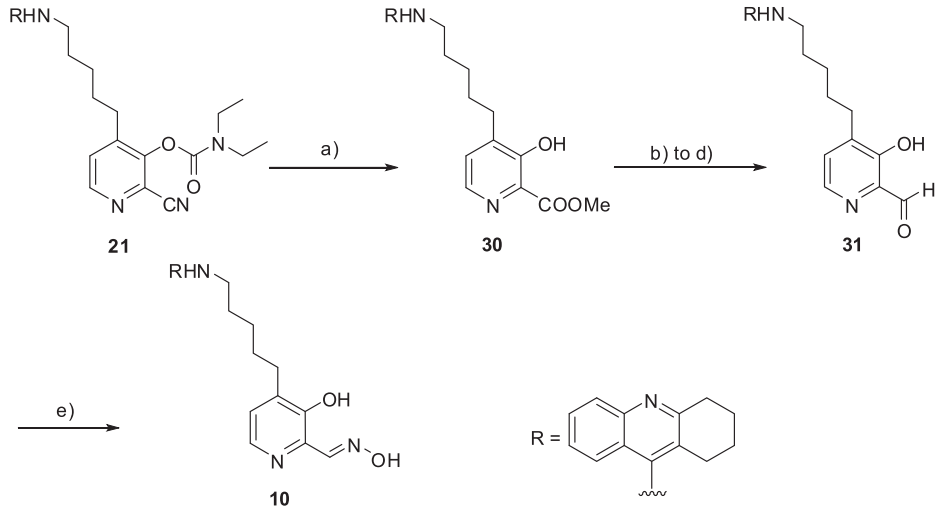

Reagents and conditions: a) MeOH, H_2SO_4, reflux, 24 h, **42%**; b) TBDMSCl, DMF, rt; c) DIBAL-H,CH_2Cl_2, -78°C; d) TBAF, THF, 0°C, **33%** over 3 steps; e) NH_2OH.HCl, CH_3COONa, EtOH, **51%**.

Scheme 4. Synthesis of oxime **10**.

The 5- and 6-substituted α-hydroxypyridine oximes analogues **11**–**13** were obtained using the modular synthetic approach, consisting in the Sonogashira coupling reaction of 6-bromopyridine **32** [17] or 5-bromopyridine **33** [30] with alkynes **19** or **34** [31], respectively, followed by reduction of the alkyne and finally *O*-debenzylation. The subsequent three-step transformation of methyl ester to aldehyde, ensued by reaction with hydroxylamine (Scheme 5), yielded the desired α-hydroxypyridine oximes **11**–**13** in 15, 28 and 18% yields.

3.3. Synthesis of 1,2,3,4-tetrahydro-9-thioacridine α-hydroxypyridine aldoxime

In order to tune the affinity of hybrid reactivator for hAChE, the structure of the PSL was changed by the substitution of NH at position 9 of 1,2,3,4-tetrahydroacridine with a sulphur atom. In short, conjugate **14** bearing 1,2,3,4-tetrahydro-9-thioacridine as PSL was synthesized according to Scheme 6 by alkylating 1,2,3,4-tetrahydro-9-thioacridine **44** [32] with **45** to give **46**, which was then used for Sonogashira coupling reaction with **47** to provide compound **48**. Contrary to **35**–**37**, the attempts to reduce the triple bond of **48** using Pd/C or $Pd(OH)_2$/C failed, possibly due to the poisoning of catalyst by the reaction with thioether groups. The use of only 1.5 equiv of PtO_2 yet resulted in successful hydrogenation, allowing to obtain compound **49** with 64% yield. The further three-step sequence comprising protection of the phenol group, reduction of methyl ester with DIBAL-H into aldehyde, and the following deprotection using TBAF generated the desired aldehyde **50**, with 42% yield. Finally, reaction of **50** with NH_2OH resulted in the formation of pyridinaldoxime **14**, with 6% overall yield.

4. Docking and molecular dynamics simulations

Ternary complexes between VX-inhibited hAChE and 3-hydroxypyridine aldoxime with 2, 3, 4 (compound **12**) or 5 (compound **11**) carbons linker were investigated by molecular docking and molecular dynamics simulations (see Supporting Information). Flexible docking experiments were undertaken, in which the side chains of active site gorge residues key to the binding of the reactivators were allowed to wander from their native position (see

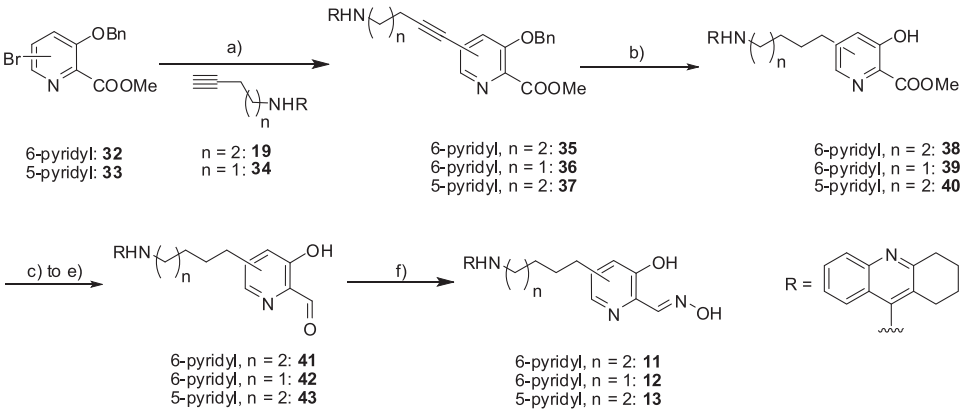

Reagents and conditions: a) **19** or **34**, $Pd(PPh_3)_4$, CuI, Et_3N, THF, 20°C, **78-98%** ; b) H_2, $Pd(OH)_2$/C, MeOH, **89-96 %**; c) TBDMSCl, DMF, rt; d) DIBAL-H, CH_2Cl_2, -78°C; e) TBAF, THF, 0°C, **43%-54%** over 3 steps; f) NH_2OH.HCl, CH_3COONa, EtOH, **55%-62%**.

Scheme 5. Synthesis of oximes **11**, **12**, and **13**.

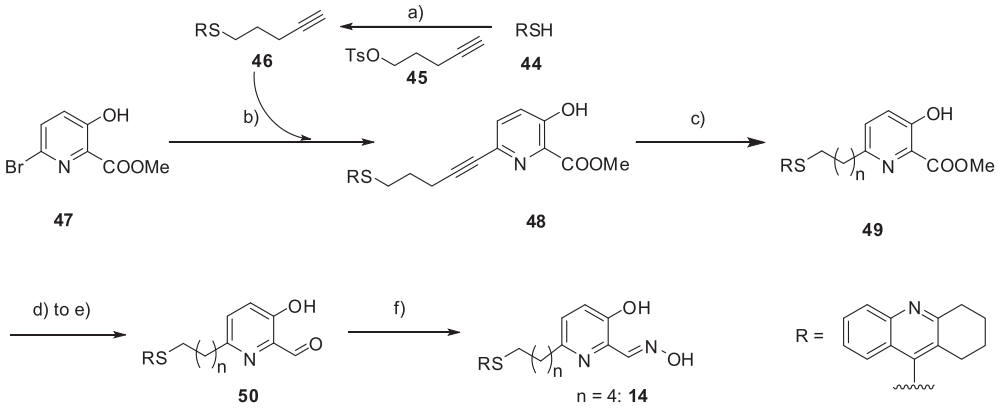

Reagents and conditions: a) **45**, $(n\text{-Bu})_4NBr$, 50% aq. NaOH, THF/H_2O, **56%**; b) **46**, $Pd(PPh_3)_2Cl_2$, CuI, Et_3N, THF, 50°C, **90%**; c) H_2, PtO_2, 5 atm, AcOEt, rt, **64 %**; d) TBDMSCl, DMF, rt; d) DIBAL-H, CH_2Cl_2, -78°C; e) TBAF, THF, 0°C, **42%** over 3 steps; f) $NH_2OH.HCl$, CH_3COONa, EtOH, **57%**.

Scheme 6. Synthesis of oxime **14**.

Supporting Information). In all four docking experiments, a conformational change was observed in the side chain of peripheral-site Trp286 (Fig. 7), faithfully reproducing the crystallographic observation from the bis-tacrine/*Tc*AChE complex (PDB code 2CEK) [19]. This conformational change results in a π–π sandwiching of the tacrine moiety between the aromatic side chains of Tyr72 and Trp286. The scoring function of the docking algorithm yielded similar binding energies for the 4 molecules of about − 9 kcal/mol, indicating that the linker is sufficiently long to prevent unproductive binding of the reactivators in the gorge of the inhibited enzyme.

The structures resulting from the 4 independent dockings were then subjected to molecular dynamics (MD) simulations for 5 ns at a temperature of 300 K. For each, the distance between the aldoxime oxygen and the VX-AChE phosphorus atom was monitored along the simulation trajectory and the distributions of distances were analyzed (Fig. 8). The shorter the distance, the higher the probability to form a covalent bond between the reactivator oxygen and the phosphorus atom, that is, the more likely should reactivation occur at a fast rate. Molecule **12** brings the aldoxime oxygen closer to the phosphorus atom and more frequently (Fig. 8), suggesting that a 4-carbon linker between the PSL and the aldoxime is optimum for reactivation.

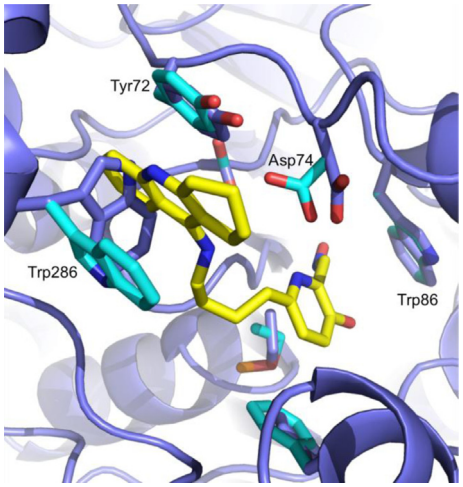

Fig. 7. Docked conformation of molecule **12** (yellow) at the peripheral site of VX-hAChE. The docked conformations of the flexible residues are shown in cyan and the native conformations (pdb code 1b41) in blue. (For interpretation of the references to colour in this figure legend, the reader is referred to the web version of this article.)

5. *In vitro* reactivation of VX-, tabun and POX-inhibited hAChE

The abilities of amidoximes **6**–**9**, as well as of aldoximes **10**–**14** to reactivate *in vitro* VX-, tabun- and ethyl-paraoxon inhibited hAChE were investigated by spectrophotometry using the Ellman's reaction. Reactivation kinetics were compared to those of known reactivators, including 2-PAM, obidoxime, HLö-7, trimedoxime (TMB4) and HI-6. 6-Substituted α-hydroxypyridine amidoxime **7** and 4-substituted α-hydroxypyridine oxime **10** were both totally inefficient in reactivating either VX-inhibited hAChE or tabun-inhibited hAChE. (Table 1)

In contrast, 4-substituted tetrahydroacridine α-hydroxypyridine amidoximes **6** (C5 alkyl linker), **8** and **9** (*N*–Me linkers) displayed improved affinity and higher reactivation efficiencies (k_{r2}) towards VX-inhibited hAChE than both 2-PAM and trimedoxime. While they remained less efficient than obidoxime, HLö-7, and HI-6 in reactivating VX-inhibited hAChE, it is noteworthy that these compounds are the first amidoxime-based reactivators that are efficient towards VX-inhibited hAChE. Quite remarkably, aldoximes **11** and **12** substituted in position 6 of the pyridine ring by the C5 and C4 alkyl linker proved more efficient in reactivating VX-inhibited hAChE than 2-PAM, obidoxime, trimedoxime, and HI-6. Although oximes **11** and **12** do not surpass the reactivating efficiency of HLö-7, nor that of our previously described compound **5a**, they represent an interesting new starting point for further improvement. It must be stressed, in particular, that since they neither bear a permanent charge nor a tertiary amine, they should be able to cross the BBB quite efficiently.

Also noteworthy is the fact that oxime **12** is able to reactivate tabun-inhibited hAChE (Table 2), an OP complex known to be reluctant to reactivation due to its weak electrophilicity and to the steric hindrance imposed on the phosphorus atom in the tabun-hAChE adduct. In fact, compound **12** exhibited higher *in vitro* reactivation potency than all quaternary pyridinium aldoximes described to date. Despite a lower reactivation rate constant (k_r) compared to obidoxime and trimedoxime, compound **12** was 4-fold more efficient than trimedoxime, the best pyridinium aldoxime reactivator of tabun-inhibited hAChE. Again, this increase in

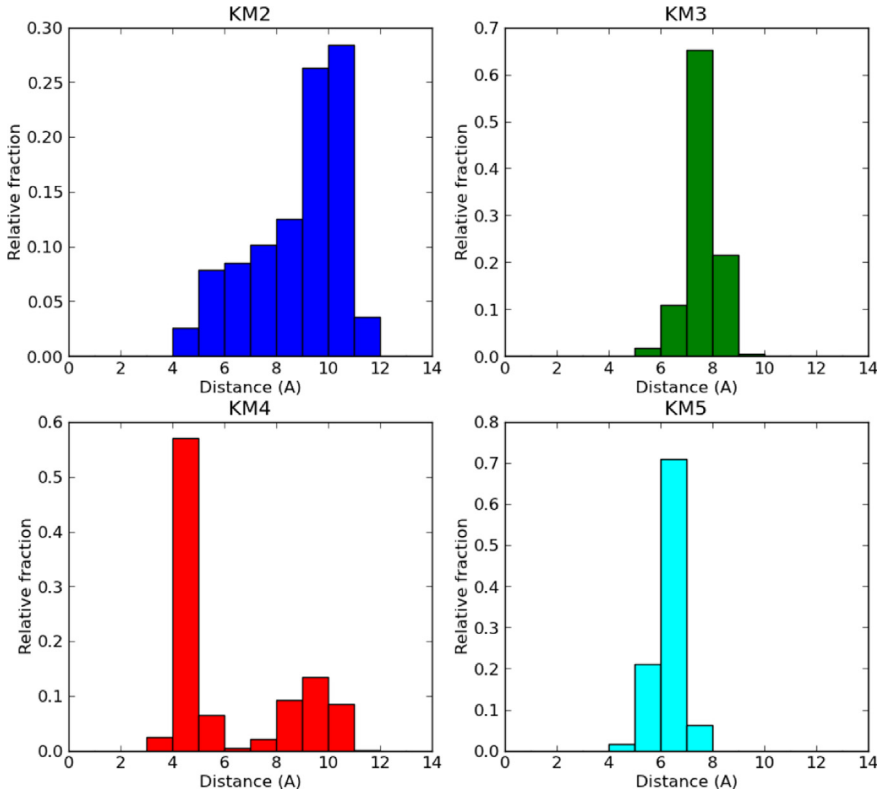

Fig. 8. Distribution of distances between the aldoxime oxygen and the VX phosphorus analyzed along the simulation trajectory for the four different linker lengths (KM 2: $-CH_2-CH_2-$; KM 3: $-CH_2-CH_2-CH_2-$, KM 4: $-CH_2-CH_2-CH_2-CH_2-$, **12**; KM 5: $-CH_2-CH_2-CH_2-CH_2-CH_2-$, **11**).

Table 1
In vitro reactivation of VX-hAChE.

Reactivator	k_r (min^{-1})	K_D (μM)	k_{r2} (mM^{-1} min^{-1})[b]
2-PAM	0.06 ± 0.01	215 ± 75	0.28
Obidoxime	0.60 ± 0.05	54 ± 12	11
HLö-7	0.49[a]	7.8[a]	63[a]
Trimedoxime	nd[c]	nd[c]	0.50 ± 0.02[c]
HI-6	0.44 ± 0.15	50 ± 26	9
6	nd[c]	nd[c]	0.65[c]
8	0.0094 ± 0.0004	15 ± 2	0.6
9	0.032 ± 0.001	30 ± 3	1.1
11	0.56 ± 0.12	41 ± 11	13
12	0.72 ± 0.07	31 ± 6	22
13	nd[d] (k_{obs} = 0.0038 ± 0.00006 min^{-1} at 1 μM)		
14	nd[d] (k_{obs} = 0.0076 ± 0.0005 min^{-1} at 200 μM)		

[a] From the ref. [33].
[b] $k_{r2} = k_r/K_D$.
[c] If [reactivator] $\ll K_D$, then there is a linear dependence between k_{obs} and [reactivator]: $k_{obs} = (k_r/K_D)$ [reactivator]. In this case, k_r and K_D cannot be determined, but $k_{r2} = k_r/K_D$ is the slope of the line.
[d] Not determined if k_{obs} is <0.01 min^{-1} at practical concentration.

Table 2
In vitro reactivation of tabun-hAChE.

Reactivator	k_r (min^{-1})	K_D (μM)	k_{r2} (mM^{-1} min^{-1})[a]
Obidoxime	0.04 ± 0.006	250 ± 110	0.16
HLö-7	0.020 ± 0.0007	106 ± 15	0.2
Trimedoxime	0.085 ± 0.005	145 ± 25	0.7
8	Less than 10% reactivation at 100 μM in 2 h		
9			
11	0.0075 ± 0.0005	30 ± 6	0.27
12	0.021 ± 0.001	7.1 ± 1.5	3

[a] $k_{r2} = k_r/K_D$.

efficiency is likely to be ascribed to its significantly greater affinity towards the tabun-hAChE conjugate (K_D). The better reactivity of compound **12** on both VX- and tabun-inhibited hAChE, as compared to compound **11**, suggest that a 4-carbon linker is optimum for both a good binding to the inhibited enzyme and an accurate orientation of the oxime function needed for displacing of the phosphyl or phosphoramidyl moiety.

As mentioned already, most organophosphate intoxication results from pesticide poisoning, which involves the formation of a diethylphosphoryl conjugate of hAChE. Testing molecules for their ability to reactivate ethylparaoxon-inhibited hAChE, therefore, allows evaluating them for their general efficacy against pesticide poisoning. Interestingly, compounds **11** and **12** proved more efficient than obidoxime and HLö-7 towards paraoxon-inhibited hAChE, (Table 3). Much like the trend observed in the case of VX, decreasing the linker length from 5 to 4 carbons led to a 1.5-fold increase in kr.

We note that compounds **7**, **10**, **11** and **12** are also able to inhibit native hAChE, with IC_{50} similar to tacrine and tacrine-pyridyl heterodimer **51** (Table 4). While these inhibitory properties could be envisaged as a drawback of our strategy aiming at increasing the efficacy of reactivators by increasing their affinities for the target enzyme, we argue conversely. Indeed, it remains to be proven that significant reversible inhibition of AChE at a concentration similar to that used to reactivate of OP-inhibited AChE is really problematic *in vivo*. Also, it was shown that reversible inhibitors have a protective effect on AChE, preventing its phosphylation by transiently occupying the active site [35].

Interestingly, 4-substituted pyridine aldoxime **10** showed no reactivation of VX-, tabun- and paraoxon-inhibited hAChE and a higher inhibition compared to tacrine. This is in strong contrast with 6-substituted compound **11** and suggests that 4-substitution of pyridine ring favours the binding of tacrine moiety to the

Table 3
In vitro reactivation of paraoxon-hAChE.

Reactivator	k_r (min^{-1})	K_D (μM)	k_{r2} (mM^{-1} min^{-1})[b]
Obidoxime	0.81[a]	32.2[a]	20[a]
HLö-7	0.63 ± 0.04	210 ± 31	3
Trimedoxime	0.34 ± 0.02[a]	47.8 ± 6.9[a]	17[a]
8	Less than 10% reactivation at 100 μM in 2 h		
9	nd[d] (k_{obs} = 0.0043 ± 0.0004 min^{-1} at 100 μM)		
11	0.0228 ± 0.0006	1.1 ± 0.1	20.9
12	0.111 ± 0.002	3.6 ± 0.2	31

[c]Not determined if k_{obs} is <0.01 min^{-1} at practical concentration.
[a] From the ref. [34].
[b] $k_{r2} = k_r/K_D$.

catalytic site of the enzyme, rather than at its peripheral site. The substitution of tacrine with thiotacrine as PSL resulted in three order of magnitude lower inhibition of native hAChE by model compound **52** and **14**, as compared to compounds **51** and **11**, respectively. However, oxime **14** exhibited very poor reactivation of VX-hAChE, demonstrating that the key to the improvement of the reactivation potency is finding the optimal balance between affinity of the bifunctional reactivator for the enzyme and positioning of the oxime function relative to the phosphorus atom of the OP-hAChE adduct.

6. Conclusion

We have described the synthesis and the *in vitro* biological properties of a series of novel, promising, non-permanently charged AChE reactivators, including differently substituted tacrine α-hydroxypyridine oximes and amidoximes. We demonstrated that the amidoxime function can be used as a reactivator function, and allows producing hybrid molecules that equal or surpass currently approved mono- and bis-pyridinium oximes, both in terms of reactivation efficiency and broadness of their activity spectrum. While it remains to be evaluated if the molecules are centrally active, or require further modifications to be so, this new family of oximes holds great promise for the medical treatment of OP-poisoning.

7. Experimental part

7.1. General materials and methods

All reactions were carried out in a flame dried glassware under an argon atmosphere with dry solvents, under anhydrous conditions unless otherwise indicated. The chemicals used in the synthesis and solvents were purchased from Aldrich, Acros, Alfa-Aesar or ABCR and used without further purification. Thin layer chromatographies (TLC) were carried out using Merck silica gel plates (silica gel 60 F_{254}). TLC plates were visualized using UV light (254 nm), followed by detection with cerium sulphate and ninhydrin. The column chromatographies were performed using Merck silica gel 60 (0.063–0.200 mm, 70–230 mesh, ASTM) according to a standard procedure. Analytical HPLC chromatography (purity >95%) were performed using SPD-20A Shimadzu apparatus equipped with a Zorbax 300SB-C18 column, using a mixture of acetonitrile and water as eluent (0.1% TFA). ^{1}H NMR and ^{13}C NMR spectra were recorded on Brucker DPX300, DPX400 and DPX500. Chemical shifts (δ) are quoted in parts per million and are calibrated relative to solvent residual peaks. Multiplicities are reported as follows: s = singlet, d = doublet, t = triplet, m = multiplet, q = quartet, qui = quintet. Coupling constant are reported in Hertz. Mass spectra were recorded on an MS/MS high resolution Micromass ZABSpecTOF spectrometer.

7.2. General procedures and analytical data of key compounds ***35***, ***36***, ***38***, ***39***, ***41***, ***42***, ***11***, and ***12***

General procedure 1 for the Sonogashira coupling reaction (synthesis of compounds **20**, **23**, **35**, **36**, and **37**). The flask containing solution of iodo- or bromopyridine (1 equiv) in THF/Et_3N was evacuated and filled with Ar three times before the addition of catalysts $Pd(PPh_3)_4$ (0.1 equiv) and CuI (0.2 equiv). After degazation with Ar the mixture was stirred at the room temperature for 5 min, then the degazed solution of alkyne (1.1 equiv) was added and the reaction mixture was stirred during 20 h at the room temperature. After concentration at reduced pressure the residue was purified by the column chromatography.

General procedure 2 for *N*-(diethylamino)carbamate group removal and nitrile conversion to amidoxime (synthesis of compounds **6**, **8**, and **9**). The solution of **21**, **28** or **29** (1 equiv), $NH_2OH.HCl$ (30 equiv), and pyridine (30 equiv) in 2 mL of ethanol was refluxed during 14 h. The solvent was removed in *vacuo*, the residue was subjected to preparative HPLC chromatography.

General procedure 3 for the one-pot alkyne reduction and O-debenzylation (synthesis of compounds **24**, **38**, **39**, and **40**). To the degazed solution of alkyne (1 equiv) in ethyl acetate or methanol Pearlman's catalyst $Pd(OH)_2/C$ (20%, moisture 50%, 0.3 equiv) was added. After the degazation the solution was bubbled with H_2. The reaction mixture was stirred at RT under H_2 (1 atm) during 24 h.

Table 4
Inhibition of hAChE.

Compound	IC_{50} (μM)	Compound	IC_{50} (μM)
Tacrine	0.20 ± 0.02 (Human erythrocyte AChE)[a]	**12**	1.40 ± 0.03 (hAChE)
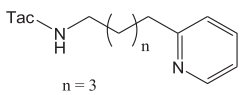 **51**	0.15 ± 0.01 (hAChE)	**13**	0.163 (hAChE)
7	0.26 ± 0.01 (hAChE)	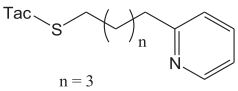 **52**	130 ± 15 (hAChE)
10	0.077 ± 0.003 (hAChE)	**14**	307 (hAChE)
11	0.26 ± 0.01 (hAChE)		

[a] From ref. [36].

The solution was filtered through celite, the solvent was evaporated, and the product was dried in *vacuo*.

General procedure 4 for the three-step transformation of the methyl ester into aldehyde (synthesis of compounds **31**, **41**, **42**, **43** and **50**). The solution of methyl ester **30**, **38**, **39**, **40** or **49** (1 equiv), imidazole (4.15 equiv), and TBDMSCl (2.4 equiv) in dry DMF was stirred at the room temperature under argon during 2 h. Ethyl acetate was added, and the organic phase was washed with water 3 times, dried over Na_2SO_4 and concentrated in *vacuum*. After drying in *vacuum* the compound obtained was subjected without purification to the following reduction of methyl ester with DIBAL-H. To the solution of the compound obtained (1 equiv) in dry CH_2Cl_2 at −78 °C DIBAL-H (1 M solution in CH_2Cl_2, 2 equiv) was added dropwise. The reaction mixture was stirred at −78 °C for 12 min, then it was quenched with MeOH, and the cooling bath was removed. When the mixture was warmed to the room temperature, the organic phase was washed with aqueous solution of NaOH (1 M), dried over Na_2SO_4 and concentrated under reduced pressure. After drying in *vacuum* the product obtained was subjected to the following reaction with TBAF. To the solution of the compound obtained (1 equiv) in dry THF at 0 °C TBAF (1 M solution in THF, 1.1 equiv) was added, and the reaction mixture was stirred at this temperature for 1 h. After removal of the solvent under reduced pressure the residue was purified by the column chromatography (silica gel).

General procedure 5 for synthesis of oximes **10**–**14.** The solution of aldehyde **31**, **41**, **42, 43** or **50** (1 equiv), $NH_2OH.HCl$ (1.5 equiv), and CH_3COONa (1.5 equiv) in dry ethanol was stirred during 8 h. After concentration under reduced pressure the crude product was purified by the column chromatography or preparative HPLC.

*7.2.1. Methyl 3-(benzyloxy)-6-{5-[(1,2,3,4-tetrahydroacridin-9-yl) amino]pent-1-yn-1-yl}pyridine-2-carboxylate (**35**)*

Compound **35** was obtained accordingly to the ***general procedure 1*** for Sonogashira coupling using **32** (0.147 g, 0.46 mmol, 1 equiv), **19** (0.132 g, 0.5 mmol, 1.1 equiv), $Pd(PPh_3)_4$ (0.041 g, 0.046 mmol, 0.1 equiv), CuI (0.017 g, 0.09 mmol, 0.2 equiv), Et_3N (3 mL), and THF (6 mL). The crude product was purified by the column chromatography (silica gel, gradient from ethyl acetate to ethyl acetate/MeOH = 8/2, R_f = 0.24). Yield 180 mg, 78%. ^{1}H NMR (300 MHz, $CDCl_3$, δ): 1.76–1.84 (4H, m), 1.87–1.97 (2H, qui, J = 6.7 Hz), 2.49 (2H, *t*, J = 6.7 Hz), 2.64 (2H, m), 3.03 (2H, m), 3.67 (2H, *t*, J = 6.9 Hz), 3.88 (3H, s, CH_3O), 5.14 (2H, s, $PhCH_2O$), 7.18–7.38 (8H, m, ArH), 7.48 (1H, *t*, J = 7.6 Hz), 7.90–7.93 (2H, m). ^{13}C NMR (100 MHz, $CDCl_3$, δ): 17.29; 22.79; 23.13; 25.05; 29.98; 33.79; 48.42; 52.88; 71.10; 80.64; 88.84; 120.24; 121.96; 122.93; 124.19; 127.12; 128.37; 128.47; 128.63; 128.75; 128.83; 128.95; 130.11; 132.24; 132.34; 135.23; 135.66; 146.91; 150.97; 153.20; 158.23; 164.99.

*7.2.2. Methyl 3-hydroxy-6-{5-[(1,2,3,4-tetrahydroacridin-9-yl) amino]pentyl}pyridine-2-carboxylate (**38**)*

Compound **38** was obtained accordingly to the ***general procedure 3*** for the reduction of the triple bond and O-debenzylation using **35** (0.180 g, 0.35 mmol), $Pd(OH)_2$/C (20%, 0.075 g, 0.11 mmol, 0.3 equiv), and 2.5 mL of MeOH. Yield 0.140 g, 94%. R_f = 0.34 (CH_2Cl_2/MeOH = 10/1). ^{1}H NMR (300 MHz, $CDCl_3$, δ): 1.40–1.50 (2H, m), 1.67–1.78 (4H, m), 1.87–1.92 (4H, m), 2.63 (2H, m), 2.78 (2H, *t*, J = 7.9 Hz), 3.11 (2H, m), 3.56 (2H, *t*, J = 7.2 Hz), 4.00 (3H, s, CH_3O), 7.23 (1H, d, J = 8.6 Hz), 7.28 (1H, d, J = 8.6 Hz), 7.31–7.36 (1H, m), 7.54–7.59 (1H, m), 7.95 (1H, d, J = 8 Hz), 8.05 (1H, d, J = 8.6 Hz). ^{13}C NMR (100 MHz, $CDCl_3$, δ): 20.87; 22.11; 23.78; 26.38; 28.60; 29.62; 31.09; 37.02; 48.61; 53.55; 110.88; 115.99; 121.66; 124.19; 125.49; 127.88; 129.65; 132.63; 139.27; 152.03; 153.45; 155.55. HRMS (ESI, *m/z*): calcd. for $C_{25}H_{30}N_3O_3$ $[M + H]^+$, 420.22871; found, 420.22836.

*7.2.3. 3-Hydroxy-6-{5-[(1,2,3,4-tetrahydroacridin-9-yl)amino] pentyl}pyridine-2-carbaldehyde (**41**)*

Compound **41** was obtained by the ***general procedure 4*** from **38** with yield 37% (over three steps). R_f = 0.23 (ethyl acetate/MeOH = 10/3). ^{1}H NMR (400 MHz, $CDCl_3$, δ): 1.40–1.48 (2H, m), 1.67–1.79 (4H, m), 1.85–1.90 (4H, m), 2.64 (2H, m), 2.76 (2H, *t*, J = 7.7 Hz), 3.05 (2H, m), 3.52 (2H, *t*, J = 7.3 Hz), 7.23 (1H, d, J = 8.7 Hz), 7.25 (1H, d, J = 8.7 Hz), 7.29–7.33 (1H, m, ArH), 7.51–7.55 (1H, m, ArH), 7.92–7.95 (2H, m), 9.99 (1H, s, CHO). ^{13}C NMR (100 MHz, $CDCl_3$, δ): 22.73; 23.11; 24.88; 26.70; 29.48; 31.76; 33.48; 37.28; 49.45; 115.48; 123.10; 124.02; 126.64; 127.99; 129.01; 129.88; 131.06; 135.95; 151.45; 154.66; 157.23; 157.88; 198.83. HRMS (ESI, *m/z*): calcd. for $[M + H]^+$, $C_{24}H_{28}N_3O_2$, 390.21815; found, 390.21892.

*7.2.4. 2-[(1E)-(hydroxyimino)methyl]-6-{5-[(1,2,3,4-tetrahydroacridin-9-yl)amino]pentyl}pyridin-3-ol (**11**)*

Compound **11** was obtained accordingly to the ***general procedure 5*** using **41** (0.050 g, 0.13 mmol, 1 equiv), $NH_2OH.HCl$ (0.013 g, 0.19 mmol, 1.5 equiv), CH_3COONa (0.016 g, 0.19 mmol, 1.5 equiv), and 1.2 mL of ethanol. After evaporation of the solvent and purification by column chromatography (ethyl acetate/MeOH = 8/2) product was obtained with yield 55%. R_f = 0.44 (ethyl acetate/MeOH = 2/1). ^{1}H NMR (400 MHz, CD_3OD, δ): 1.37–1.44 (2H, m, CH_2), 1.68–1.76 (2H, qui, J = 7.4 Hz, CH_2), 1.77–1.85 (2H, qui, J = 7.4 Hz, CH_2), 1.90–1.94 (4H, qui, J = 3.3 Hz, CH_2), 2.63 (2H, m, CH_2), 2.70 (2H, *t*, J = 7.4 Hz, CH_2), 3.00 (2H, m, CH_2), 3.87 (2H, *t*, J = 6.9 Hz, CH_2), 7.08 (1H, d, J = 8.4 Hz, ArH), 7.20 (1H, d, J = 8.4 Hz, ArH), 7.50–7.54 (1H, m, ArH), 7.76–7.81 (2H, m, ArH), 8.17 (1H, s, N=CH), 8.30 (1H, d, J = 8.7 Hz). ^{13}C NMR (100 MHz, CD_3OD, δ): 22.31; 23.30; 25.25; 27.05; 30.30; 30.53; 30.91; 31.42; 37.56; 117.95; 121.70; 125.51; 126.08; 126.18; 133.42; 136.35; 152.90; 153.85; 154.49. MS *m/z* (ESI) calcd. for $C_{24}H_{29}N_4O_2$ $[M + H]^+$, 405.22; found, 405.2.

*7.2.5. Methyl 3-(benzyloxy)-6-{4-[(1,2,3,4-tetrahydroacridin-9-yl) amino]but-1-yn-1-yl}pyridine-2-carboxylate (**36**)*

Compound **36** was obtained accordingly to the ***general procedure 1*** for Sonogashira coupling reaction using **32** (0.292 g, 0.91 mmol, 1 equiv), **34** (0.250 g, 1 mmol, 1.1 equiv), $Pd(PPh_3)_4$ (0.081 g, 0.091 mmol, 0.1 equiv), CuI (0.035 g, 0.18 mmol, 0.2 equiv), Et_3N (6 mL), and THF (12 mL). The crude product was purified by the column chromatography (silica gel, gradient from ethyl acetate/MeOH = 10/1 to ethyl acetate/MeOH = 8/2), R_f = 0.43 (ethyl acetate/MeOH = 4/1). Yield 0.440 g, 98%. ^{1}H NMR (400 MHz, $CDCl_3$, δ): 1.82–1.89 (4H, m), 2.67 (2H, *t*, J = 6.3 Hz), 2.79 (2H, *t*, J = 5.9 Hz), 3.06 (2H, *t*, J = 5.9 Hz), 3.70–3.75 (2H, dt, J = 6.4 Hz), 3.95 (3H, s), 4.48 (1H, *t*, J = 6.4 Hz, NH), 5.19 (2H, s, OCH_2Ph), 7.25 (1H, d, J = 8.8 Hz), 7.28 (2H, d, J = 8.8 Hz), 7.31–7.42 (6H, m, ArH), 7.52–7.56 (1H, m), 7.97 (2H, *t*, ArH, J = 8.3 Hz). ^{13}C NMR (100 MHz, $CDCl_3$, δ): 22.10; 22.59; 22.99; 24.93; 29.89; 33.29; 47.34; 52.93; 71.10; 77.43; 81.98; 86.71; 116.94; 120.15; 121.92; 123.00; 124.56; 127.14; 127.66; 128.51; 128.97; 129.30; 130.09; 134.74; 135.59; 140.67; 146.04; 151.08; 153.37; 157.78; 164.98. HRMS (ESI, *m/z*): calcd. for $C_{31}H_{30}N_3O_3$ $[M + H]^+$, 492.22871; found, 492.22851.

*7.2.6. Methyl 3-hydroxy-6-{4-[(1,2,3,4-tetrahydroacridin-9-yl) amino]butyl}pyridine-2-carboxylate (**39**)*

Compound **39** was obtained accordingly to the ***general procedure 3*** using **36** (0.43 g, 0.87 mmol), $Pd(OH)_2$/C (20%, 0.184 g, 0.26 mmol, 0.3 equiv), and 3 mL of MeOH. Yield 0.34 g, 96%. R_f = 0.43 (CH_2Cl_2/MeOH = 10/1). ^{1}H NMR (300 MHz, CD_3OD, δ): 1.67–1.74 (4H, m), 1.87–1.91 (4H, m), 2.68 (2H, *t*, J = 5.3 Hz), 2.72 (2H, *t*, J = 7 Hz), 2.96 (2H, *t*, J = 5.5 Hz), 3.62 (2H, *t*, J = 6.7 Hz), 3.96 (3H, s, CH_3O), 7.23 (1H, d, J = 8.6 Hz), 7.27 (2H, d, J = 8.6 Hz), 7.34–

7.40 (1H, m), 7.57–7.62 (1H, m), 7.74 (1H, d, $J = 8.4$ Hz), 8.10 (1H, d, $J = 8.4$ Hz). ^{13}C NMR (100 MHz, CD_3OD, δ): 23.25; 23.87; 25.96; 28.22; 31.31; 32.84; 37.27; 53.34; 115.73; 120.15; 125.07; 125.29; 125.74; 128.52; 130.46; 130.65; 131.09; 145.48; 154.49; 154.54; 156.94; 158.65; 170.62. HRMS (ESI, *m/z*): calcd. for $C_{24}H_{28}N_3O_3$ $[M + H]^+$, 406.21306; found, 406.21307.

7.2.7. 3-Hydroxy-6-{4-[(1,2,3,4-tetrahydroacridin-9-yl)amino] butyl}pyridine-2-carbaldehyde (**42**)

Compound **42** was obtained from **39** accordingly to the ***general procedure 4*** after purification by the column chromatography (silica gel, ethyl acetate/MeOH = 8/2) with yield 54% (over 3 steps). $R_f = 0.21$ (ethyl acetate/MeOH = 7/3). ^{1}H NMR (400 MHz, $CDCl_3$, δ): 1.66–1.75 (2H, m), 1.78–1.89 (6H, m), 2.67 (2H, m), 2.79 (2H, *t*, $J = 7$ Hz), 3.04 (2H, m), 3.52 (2H, *t*, $J = 7$ Hz), 7.20 (1H, d, $J = 8.6$ Hz), 7.24 (1H, d, $J = 8.6$ Hz), 7.31 (1H, td, $J = 6.8$ Hz, $J = 1$ Hz), 7.53 (1H, td, $J = 6.8$ Hz, $J = 1$ Hz), 7.89–7.93 (2H, m), 9.98 (1H, s, CH=O). ^{13}C NMR (100 MHz, $CDCl_3$, δ): 22.89; 23.20; 25.01; 26.96; 31.37; 33.92; 36.98; 49.32; 116.06; 120.29; 122.94; 123.95; 126.69; 128.68; 129.87; 136.00; 147.27; 150.99; 154.29; 157.29; 158.43; 198.74. HRMS (ESI, *m/z*): calcd. for $C_{23}H_{26}N_3O_2$ $[M + H]^+$, 376.20250; found, 376.20201.

7.2.8. 2-[1-(Hydroxyimino)methyl]-6-{4-[(1,2,3,4-tetrahydroacridin-9-yl)amino]butyl}pyridin-3-ol (**12**)

Compound **12** was obtained accordingly to the ***general procedure 5*** using **42** (0.090 g, 0. 24 mmol, 1 equiv), $NH_2OH.HCl$ (0.025 g, 0.36 mmol, 1.5 equiv), CH_3COONa (0.029 g, 0.36 mmol, 1.5 equiv), and 2.5 mL of ethanol. Compound **12** was purified by the column chromatography (silica gel, CH_2Cl_2/MeOH = 8/2) with yield 55%. $R_f = 0.6$ (ethyl acetate/MeOH = 2/1). ^{1}H NMR (400 MHz, CD_3OD, δ): 1.80–1.83 (4H, m, $CH_2CH_2CH_2CH_2$), 1.90–1.95 (4H, m, $CH_2CH_2CH_2CH_2$), 2.62 (2H, *t*, $J = 5.5$ Hz, CH_2), 2.71 (2H, *t*, $J = 6.4$ Hz, CH_2), 2.98 (2H, m, CH_2), 3.87 (2H, *t*, $J = 5.6$ Hz, CH_2), 7.04 (1H, d, $J = 8.4$ Hz, ArH), 7.09 (1H, d, $J = 8.4$ Hz); 7.47–7.51 (1H, m, ArH), 7.71–7.79 (2H, m, ArH), 8.08 (1H, s, CH=N), 8.24 (1H, d, $J = 8.8$ Hz). ^{13}C NMR (100 MHz, CD_3OD, δ): 22.04; 23.09; 25.03; 27.55; 29.84; 30.60; 37.11; 113.35; 117.54; 121.08; 125.43; 125.83; 126.12; 126.19; 133.51; 136.24; 140.59; 152.44; 152.75; 153.65; 154.12; 157.25. HRMS (ESI, *m/z*): calcd. for $C_{23}H_{27}N_4O_2$ $[M + H]^+$ 391.21340; found, 391.21337.

7.3. Biological essays

7.3.1. IC_{50} measurements

Recombinant hAChE was produced and purified as previously described (see reference: http://www.ncbi.nlm.nih.gov/pubmed/18975951). Oximes were dissolved in MeOH to make 5- or 10-mM stock solution. Recombinant hAChE activity was measured spectrophotometrically (absorbance at 412 nm) in the presence of various concentrations of oximes in 1 mL Ellman's buffer (phosphate 0.1 M, pH 7.4, 0.1% BSA, 5% MeOH, 0.5 mM DTNB, 25 °C). Measurements were performed at least in duplicate for each concentration tested. The concentration of oxime producing 50% of enzyme inhibition was determined by non-linear fitting using ProFit (Quantumsoft) using the standard IC_{50} equation: % Activity = 100*IC_{50}/(IC_{50} + [Ox]).

7.3.2. Inhibition of hAChE by OPs

VX, tabun were from DGA maîtrise NRBC (Vert le Petit, France). Paraoxon-ethyl was purchased from Sigma–Aldrich. Stock solution of VX and tabun were 5 mM in isopropanol. The inhibition of 120 μM hAChE is realized with a 5-fold excess of OPs and was performed in tris buffer (20 mM, pH 7.4, 0.1% BSA) at 25 °C. After a 20-min incubation, inhibited hAChE was desalted on PD-10 column (GE Healthcare).

7.3.3. Reactivation of hAChE inhibited by OPs

Hlö-7 was from DGA maîtrise NRBC (Vert le Petit, France), HI-6 from Pharmacie Centrale des Armées (Orléans, France) and obidoxime was from CRSSA (Lyon, France; synthesized by Bernard Desiré). OP-inhibited hAChE was incubated at 37 °C with at least 4 concentrations of oxime in phosphate buffer (0.1 M, pH 7.4, 0.1% BSA). The final concentration of MeOH in the incubation mix was below 2% and had no influence on the enzyme stability. At time intervals ranging from 1 to 10 min depending on the reactivation rate, 10-μL aliquots of each solutions containing the different concentrations of oxime were transferred to cuvettes containing 1 mM acetylthiocholine in 1 mL Ellman's buffer (phosphate 0.1 M, pH 7.4, 0.1% BSA, 0.5 mM DTNB, 25 °C) for measurement of hAChE activity. The enzyme activity in the control (uninhibited enzyme + oxime) remained constant during the experiment. Oximolysis was undetectable.

The percentage of reactivated enzyme (%E_{react}) was calculated as the ratio of the recovered enzyme activity and activity in the control. The apparent reactivation rate k_{obs} for each oxime concentration, the dissociation constant K_D of inhibited enzyme–oxime complex (E–PO_x) and the maximal reactivation rate constant k_r, were calculated by non-linear fit with ProFit (Quantumsoft) using the standard oxime concentration-dependent reactivation equation derived from the following scheme:

$$E - P + \mathrm{Ox} \overset{K_D}{\rightleftarrows} E - \mathrm{POx} \xrightarrow{k_r} E + \mathrm{POx}$$

$$\%E_{\mathrm{react}} = 100 \cdot \left(1 - e^{k_{\mathrm{obs}} \cdot t}\right) \quad \text{and} \quad k_{\mathrm{obs}} = \frac{k_r[\mathrm{Ox}]}{K_D + [\mathrm{Ox}]}$$

Detailed reactivator concentrations used for each set of experiments are given in the Supplementary Information.

7.4. Molecular modelling

Flexible dockings have been performed using autodock vina [37] and by preparing the system in PyMOL (Schrödinger) using the plug-in developed by Daniel Seeliger (http://wwwuser.gwdg.de/~dseelig/adplugin.html). VX-hAChE was constructed from the apo form (pdb code 4EY4) by homology to the mAChE-VX structure (pdb code 2Y2U), keeping in the active site all the usually conserved water molecules. Residues in the gorge (Tyr72, Asp74, Trp86, Tyr124, Ser125, Trp286, Tyr337, Phe338, Tyr341) have been chosen as flexible, along with the ethyl group of VX. A docking box of 60 × 60 × 60 Å was chosen, centered at the bottom of the gorge between Tyr124 and Trp86. Ligands were built and optimized from SMILEs string using Phenix elbow [38]. The default parameter set of Autodock vina was used to generate 9 docking poses per molecule.

Molecular dynamics simulations were carried out using GROMACS 4.5.6 [39] and the Amber99sb forcefield [40]. The topological description of each KM molecule was built using acpype and the general amber forcefield [41]. The hAChE-VX complex in the conformation obtained from flexible dockings together with crystal water molecules and the different KM molecules, was immersed in a periodic water box of cubic shape with a minimal distance of 10 Å to any edge and periodic boundary conditions. The box was solvated using the TIP3P solvation model and chloride and sodium counter ions were added to neutralize the simulation system. After energy minimization using a 500-step steepest decent method, the system was subjected to equilibration at 1 bar for 50 ps under the conditions of position restraints for heavy atoms. The solvent, the counter ions, and the protein were coupled separately to a temperature bath at 300 K. The Lennard–Jones interactions were cutoff at 1.4 nm. The long-range electrostatic interactions

were handled using particle-mesh Ewald method for determining long-range electrostatics (9 Å cutoff). Temperature was set to 300 K and was kept constant using a Berendsen thermostat [42] (with a coupling time constant of 0.1 ps). Pressure with a reference value of 1 bar was controlled by a Berendsen barostat (with a coupling time constant of 1 ps and a compressibility of 4.5 10^5 bar). Full MD simulation was performed for 5 ns at 300 K, using 2 fs timesteps. All bond lengths were constrained using the LINCS algorithm allowing an integration step of 2 fs [43]. Coordinates were saved every 250 steps (every 0.5 ps).

Acknowledgements

The ANR (Detoxneuro ANR-06-BLAN-163, ReAChE ANR-09-BLAN-192), DGA (DGA/STTC PDH-2-NRBC-4-C-403, DGA-REI 2009-34-0023) and DTRA (HDTRA1-11-C-0047) are gratefully acknowledged for financial support. This work has been partially supported by INSA Rouen, Rouen University, CNRS, Labex SynOrg (ANR-11-LABX-0029) and région Haute-Normandie (CRUNCh network). We also thank Dr. Patrick Wehrung, Pascale Buisine and Cyril Antheaume (UdS, Faculty of Pharmacy, Service Commun d'Analyse) for mass and NMR analyses.

Appendix A. Supplementary data

Supplementary data related to this article can be found at http://dx.doi.org/10.1016/j.ejmech.2014.03.044.

References

[1] (a) P. Taylor, Goodman, Gilman's, in: J.G. Hardman, L.E. Limbird, A.G. Goodman (Eds.), The Pharmacological Basis of Therapeutics, tenth ed., McGraw-Hill, New York, 2001, p. 175;
(b) R.E. Langford, Introduction to Weapons of Mass Destruction, Radiological, Chemical and Biological, Wiley, New York, 2004.
[2] (a) T.C. Marrs, Organophosphate poisoning, Phamacology Therapy 58 (1993) 51–66;
(b) F.R. Sidell, J. Borak, Chemical warfare agents: II. Nerve agents, Annals of Emergency Medicine 21 (1992) 865–871.
[3] Convention on the Prohibition of the Development, Production, Stockpiling and Use of Chemical Weapons and on Their Destruction; the Technical Secretariat of the Organization for the Prohibition of Chemical Weapons, Den Hague, Netherlands, 1993.
[4] M. Eddleston, N.A. Buckley, P. Eyer, A.H. Dawson, Management of acute organophosphorus pesticide poisoning, Lancet 371 (2008) 597–607.
[5] M. Eddleston, L. Karalliedde, N. Buckley, R. Fernando, G. Hutchinson, G. Isbister, F. Konradsen, D. Murray, J.C. Piola, N. Senanayake, R. Sheriff, S. Singh, S.B. Siwach, L. Smit, Pesticide poisoning in the developing world – a minimum pesticides list, Lancet 360 (2002) 1163–1167.
[6] G. Mercey, T. Verdelet, J. Renou, M. Kliachyna, R. Baati, F. Nachon, L. Jean, P.-Y. Renard, Reactivators of acetylcholinesterase inhibited by organophosphorus nerve agents, Accounts of Chemical Research 45 (2012) 756–766.
[7] D.E. Lorke, H. Kalasz, G.A. Petroianu, K. Tekes, Entry of oximes into the brain: a review, Current Medicinal Chemistry 15 (2008) 743–753.
[8] K. Sakurada, K. Matsubara, K. Shimizu, H. Shiono, Y. Seto, K. Tsuge, M. Yoshino, I. Sakai, H. Mukoyama, T. Takatori, Pralidoxime iodide (2-PAM) penetrates across the blood-brain barrier, Neurochemical Research 28 (2003) 1401–1407.
[9] T.M. Shih, J.W. Skovira, J.C. O'Donnell, J.H. McDonough, Central acetylcholinesterase reactivation by oximes improves survival and terminates seizures following nerve agent intoxication, Advanced Studies in Biology 1 (2009) 155–196.
[10] M.C. de Koning, M. van Grol, D. Noort, Peripheral site ligand conjugation to a non-quaternary oxime enhances reactivation of nerve agent-inhibited human acetylcholinesterase, Toxicology Letters 206 (2011) 54–59.
[11] (a) Z. Radić, R.K. Sit, Z. Kovarik, S. Berend, E. Garcia, L. Zhang, G. Amitai, C. Green, B. Radić, V.V. Fokin, K.B. Sharpless, P. Taylor, Refinement of structural leads for centrally acting oxime reactivators of phosphylated cholinesterases, Journal of Biological Chemistry 287 (2012) 11798–11809;
(b) R.K. Sit, Z. Radić, V. Gerardi, L. Zhang, E. Garcia, M. Katalinić, G. Amitai, Z. Kovarik, V.V. Fokin, K.B. Sharpless, P. Taylor, New structural scaffolds for centrally acting oxime reactivators of phosphylated cholinesterases, Journal of Biological Chemistry 286 (2011) 19422–19430.
[12] (a) J. Kalisiak, E.C. Ralph, J. Zhang, J.R. Cashman, Amidine-oximes: reactivators for organophosphate exposure, Journal of Medicinal Chemistry 54 (2011) 3319–3330;
(b) J. Kalisiak, E.C. Ralph, J.R. Cashman, Nonquaternary reactivators for organophosphate-inhibited cholinesterases, Journal of Medicinal Chemistry 55 (2012) 465–474.
[13] W.P. Jencks, J. Carriuolo, Reactivity of nucleophilic reagents toward esters, Journal of the American Chemical Society 82 (1960) 1778–1786.
[14] G. Saint-André, M. Kliachyna, S. Kodepelly, L. Louise-Leriche, E. Gillon, P.-Y. Renard, F. Nachon, R. Baati, A. Wagner, Design, synthesis, and evaluation of new alpha-nucleophiles for the hydrolysis of organo-phosphorus nerve agents: application to the reactivation of phosphorylated AChE, Tetrahedron 67 (2011) 6352–6361.
[15] L. Louise-Leriche, E. Păunescu, G. Saint-André, R. Baati, A. Romieu, A. Wagner, P.-Y. Renard, A HTS assay for the detection of organophosphorus nerve agent scavengers, Chemistry European Journal 16 (2010) 3510–3523.
[16] A. Krasiński, Z. Radić, R. Manetsch, J. Raushel, P. Taylor, K.B. Sharpless, H.C. Kolb, In situ selection of lead compounds by click chemistry: target-guided optimization of acetylcholinesterase inhibitors, Journal of the American Chemical Society 127 (2005) 6686–6692.
[17] (a) G. Mercey, T. Verdelet, G. Saint-André, E. Gillon, A. Wagner, R. Baati, L. Jean, F. Nachon, P.-Y. Renard, First efficient uncharged reactivators for the dephosphylation of poisoned human acetylcholinesterase, Chemical Communications 47 (2011) 5295–5297;
(b) G. Mercey, J. Renou, T. Verdelet, M. Kliachyna, R. Baati, E. Gillon, M. Arboleas, M. Loiodice, F. Nachon, L. Jean, P.-Y. Renard, Phenyltetrahydroisoquinoline-pyridinaldoxime conjugates as efficient uncharged reactivators for the dephosphylation of inhibited human acetylcholinesterase, Journal of Medicinal Chemistry 55 (2012) 10791–10795;
(c) J. Renou, M. Loiodice, M. Arboléas, R. Baati, L. Jean, F. Nachon, P.-Y. Renard, Tryptoline-3-hydroxypyridinaldoxime conjugates as efficient reactivators of phosphylated human acetyl and butyrylcholinesterases, Chemical Communications 50 (2014) 3947–3950.
[18] Y. Ashani, A.K. Bhattacharjee, H. Leader, A. Saxena, B.P. Doctor, Inhibition of cholinesterases with cationic phosphonyl oximes highlights distinctive properties of the charged pyridine groups of quaternary oxime reactivators, Biochemical Pharmacology 66 (2003) 191–202.
[19] J.P. Colletier, B. Sanson, F. Nachon, E. Gabellieri, C. Fattorusso, G. Campiani, M. Weik, Conformational flexibility in the peripheral site of *Torpedo californica* acetylcholinesterase revealed by the complex structure with a bifunctional inhibitor, Journal of the American Chemical Society 128 (2006) 4526–4527.
[20] E.H. Rydberg, B. Brumshtein, H.M. Greenblatt, D.M. Wong, D. Shaya, L.D. Williams, P.R. Carlier, Y.P. Pang, I. Silman, J.L. Sussman, Complexes of alkylene-linked tacrine dimers with *Torpedo californica* acetylcholinesterase: binding of bis5-tacrine produces a dramatic rearrangement in the active-site gorge, Journal of Medicinal Chemistry 49 (2006) 5491–5500.
[21] J.L. Sussman, M. Harel, F. Frolow, C. Oefner, A. Goldman, L. Toker, I. Silman, Atomic structure of acetylcholinesterase from *Torpedo californica*: a prototypic acetylcholine-binding protein, Science 253 (1991) 872–879.
[22] J.P. Colletier, D. Fournier, H.M. Greenblatt, J. Stojan, J.L. Sussman, G. Zaccai, I. Silman, M. Weik, Structural insights into substrate traffic and inhibition in acetylcholinesterase, Embo Journal 25 (2006) 2746–2756.
[23] Y. Bourne, P. Taylor, Z. Radic, P. Marchot, Structural insights into ligand interactions at the acetylcholinesterase peripheral anionic site, Embo Journal 22 (2003) 1–12.
[24] Y. Bourne, H.C. Kolb, Z. Radic, K.B. Sharpless, P. Taylor, P. Marchot, Freeze-frame inhibitor captures acetylcholinesterase in a unique conformation, Proceedings of the National Academy of Sciences of the United States of America 101 (2004) 1449–1454.
[25] B. Sanson, F. Nachon, J.P. Colletier, M.T. Froment, L. Toker, H.M. Greenblatt, J.L. Sussman, Y. Ashani, P. Masson, I. Silman, M. Weik, Crystallographic snapshots of nonaged and aged conjugates of soman with acetylcholinesterase, and of a ternary complex of the aged conjugate with pralidoxime, Journal of Medicinal Chemistry 52 (2009) 7593–7603.
[26] W.G. Lewis, L.G. Green, F. Grynszpan, Z. Radic, P.R. Carlier, P. Taylor, M.G. Finn, K.B. Sharpless, Click chemistry in situ: acetylcholinesterase as a reaction vessel for the selective assembly of a femtomolar inhibitor from an array of building blocks, Angewantde Chemie International Edition 41 (2002) 1053–1057.
[27] (a) T. Kawaguchi, H. Akatsuka, T. Iijima, T. Watanabe, J. Murakami, T. Mitsui, 2006, JP 2006 04 5220A.
(b) T. Kawaguchi, H. Akatsuka, T. Iijima, T. Watanabe, J. Murakami, T. Mitsui, 2004, WO 2004063202 A1.
[28] S. Butini, G. Campiani, M. Borriello, S. Gemma, A. Panico, M. Persico, B. Catalanotti, S. Ros, M. Brindisi, M. Agnusdei, I. Fiorini, V. Nacci, E. Novellino, T. Belinskaya, A. Saxena, C. Fattorusso, Exploiting protein fluctuations at the active-site gorge of human cholinesterases: further optimization of the design strategy to develop extremely potent inhibitors, Journal of Medicinal Chemistry 51 (2008) 3154–3170.
[29] C. Ronco, L. Jean, H. Outaabout, P.-Y. Renard, Palladium-catalyzed preparation of *N*-Alkylated tacrine and huprine compounds, European Journal of Organic Chemistry (2011) 302–310.
[30] T. Verdelet, G. Mercey, N. Correa, L. Jean, P.-Y. Renard, Straightforward and efficient synthesis of 3-benzyloxy-4-bromopicolinate ester and 3-benzyloxy-5-bromopicolinate ester, common building blocks for pharmaceuticals and agrochemicals, Tetrahedron 67 (2011) 8757–8762.

[31] R. Manetsch, A. Krasiński, Z. Radić, J. Raushel, P. Taylor, K.B. Sharpless, H.S. Kolb, In situ click chemistry: enzyme inhibitors made to their own specifications, Journal of the American Chemical Society 126 (2004) 12809–12818.
[32] G. Campiani, C. Fattorusso, S. Butini, A. Gaeta, M. Agnusdei, S. Gemma, M. Persico, B. Catalanotti, L. Savini, V. Nacci, E. Novellino, H.W. Holloway, N.H. Greig, T. Belinskaya, J.M. Fedorko, A. Saxena, Development of molecular probes for the identification of extra interaction sites in the mid-gorge and peripheral sites of butyrylcholinesterase (BuChE). Rational design of novel, selective, and highly potent BuChE inhibitors, Journal of Medicinal Chemistry 48 (2005) 1919–1929.
[33] F. Worek, H. Thiermann, L. Szinicz, P. Eyer, Kinetic analysis of interactions between human acetylcholinesterase, structurally different organophosphorus compounds and oximes, Biochemical Pharmacology 68 (2004) 2237–2248.
[34] F. Worek, T. Wille, M. Koller, H. Thiermann, Reactivation kinetics of a series of related bispyridinium oximes with organophosphate-inhibited human acetylcholinesterase-Structure-activity relationships, Biochemical Pharmacology 83 (2012) 1700–1706.
[35] Y. Wang, Y. Wei, S. Oguntayo, B.P. Doctor, M.P. Nambiar, A combination of [+] and [−]-Huperzine A improves protection against soman toxicity compared to [+]-Huperzine A in guinea pigs, Chemico-Biological Interactions 203 (2013) 120–124.
[36] (a) P.R. Carlier, E.S.-H. Chow, Y. Han, J. Liu, J.E. Yazal, Y.-P. Pang, Heterodimeric tacrine-based acetylcholinesterase inhibitors: investigating ligand-peripheral site interactions, Journal of Medicinal Chemistry 42 (1999) 4225–4231;
(b) P. Camps, R. El Achab, J. Morral, D. Muñoz-Torrero, A. Badia, J.E. Baños, N.M. Vivas, X. Barril, M. Orozco, F.J. Luque, New tacrine-huperzine A hybrids (huprines): highly potent tight-binding acetylcholinesterase inhibitors of interest for the treatment of Alzheimer's disease, Journal of Medicinal Chemistry 43 (2000) 4657–4666.
[37] E. Carletti, H. Li, B. Li, F. Ekström, Y. Nicolet, M. Loiodice, E. Gillon, M.-T. Froment, O. Lockridge, L.M. Schopfer, P. Masson, F. Nachon, Aging of cholinesterases phosphylated by tabun proceeds through O-dealkylation, Journal of the American Chemical Society 130 (2008) 16011–16020.
[38] P.D. Adams, P.V. Afonine, G. Bunkóczi, V.B. Chen, I.W. Davis, N. Echols, J.J. Headd, L.-W. Hung, G.J. Kapral, R.W. Grosse-Kunstleve, A.J. McCoy, N.W. Moriarty, R. Oeffner, R.J. Read, D.C. Richardson, J.S. Richardson, T.C. Terwilliger, P.H. Zwart, PHENIX: a comprehensive Python-based system for macromolecular structure solution, Acta Crystallographica D66 (2010) 213–221.
[39] B. Hess, C. Kutzner, D. van der Spoel, E. Lindahl, GROMACS 4: algorithms for highly efficient, load-balanced, and scalable molecular simulation, Journal of Chemical Theory and Computation 4 (2008) 435–447.
[40] V. Hornak, R. Abel, A. Okur, B. Strockbine, A. Roitberg, C. Simmerling, Comparison of multiple amber force fields and development of improved protein Backbone parameters, Proteins 65 (2006) 712–725.
[41] J. Wang, R.M. Wolf, J.W. Caldwell, P.A. Kollman, D.A. Case, Development and testing of a general amber force field, Journal of Computational Chemistry 25 (2004) 1157–1174.
[42] H.J.C. Berendsen, J.P.M. Postma, W.F. van Gunsteren, A. DiNola, J.R. Haak, Molecular dynamics with coupling to an external bath, Journal of Chemical Physics 81 (1984) 3684–3690.
[43] B. Hess, H. Bekker, H.J.C. Berendsen, J.G.E.M. Fraaije, LINCS: a linear constraint solver for molecular simulations, Journal of Computational Chemistry 18 (1997) 1463–1472.